Mechanism of the reverse gate leakage in AlGaN/GaN high electron mobility transistors

Shreepad Karmalkar[a] and D. Mahaveer Sathaiya
Department of Electrical Engineering, Indian Institute of Technology, Madras 600 036, India

M. S. Shur[b]
ECSE Department, Rensselaer Polytechnic Institute, CII 9015, 110 8th Street, Troy, New York 12180

The off-state gate current in AlGaN/GaN high electron mobility transistors is shown to arise from two parallel gate to substrate tunneling paths: a direct path, and a path via deep traps, which are distributed throughout the AlGaN layer and spread over an energy band. A model to calculate this current is given, which shows that trap-assisted tunneling dominates below $T \sim 500$ K, and direct tunneling (thermionic field emission) dominates at higher temperatures. A model fit to experimental results yields the following fabrication process sensitive parameters: trap concentration of $\sim 10^{13} - 10^{15}$ cm^{-3}, and trap bandwidth of $\sim 50\% - 70\%$ of the barrier height located $0.4 - 0.55$ V below the conduction band edge. © *2003 American Institute of Physics.*
[DOI: 10.1063/1.1579852]

GaN based high electron mobility transistors (HEMTs) have emerged as very attractive candidates for high-temperature, high-voltage, and high-power operation at microwave as well as lower frequencies.[1,2] Their off-state gate current, I_G, is sensitive to their fabrication process, and can be as much as two orders of magnitude more than that in GaAs based HEMTs.[3] A clear understanding of this phenomenon is urgent, to fully develop the potential of AlGaN/GaN HEMTs by lowering I_G, and therefore reducing the noise[4] and power consumption. Such an understanding may be obtained from this letter, where we provide a qualitative and quantitative account of the I_G mechanisms in AlGaN/GaN HEMTs.

We regard I_G to arise from two parallel electron transport processes, namely—trap-assisted tunneling (TT) and direct tunneling (DT) through the gate potential barrier, i.e.,

$$I_G = I_{TT} + I_{DT}. \tag{1}$$

The thermionic emission over the barrier has been ignored, since it is not significant in the temperature range for device operation.

Our proposals for the nature of traps and the TT process are shown in Fig. 1. To account for the high I_G values observed, we assume that the traps are distributed throughout the AlGaN layer and spread over an energy band located within the barrier height. It is of interest to note that, we tried a leakage current model based on tunneling via a single trap level. However, this model could only predict the current at high gate voltages as a function of temperature. Its current predictions as a function of temperature for low gate voltages showed large discrepancies, which could only be removed if the tunneling was assumed to occur via a band of traps.

Electrons can tunnel via the trap band by numerous two-step and multistep tunneling processes. The most probable of these is the two-step process in which electrons tunnel into

and out of the traps having energies close to the band edges $\phi_{1,2}$. Under steady state conditions, the rates $R_{1,2}$ of these two processes are equal, and the trap occupancy f_t within the trap band at any energy ϕ is spatially constant.

It has been pointed out[5] that the magnitude of I_G saturates for $V_G \gtrsim |V_T|$, where V_G is the reverse voltage magnitude and V_T is the device threshold voltage. This is because the vertical electric field picture beneath the gate, which controls I_G, does not change for $V_G > |V_T|$, as the extra voltage $V_G - |V_T|$ drops laterally from gate to drain/source. Note that, higher the $|V_T|$, higher is the value at which I_G saturates. Further, this saturation I_G depends on the polarization/strain charges in the AlGaN layer, since V_T is proportional to these charges.[6] As per our model, the saturation I_G is dominated by I_{TT} and I_{DT} in the low and high temperature ranges, respectively, as shown in Fig. 2.

We formulate an expression for I_{TT} as a function of $V_G \leq |V_T|$, and temperature, T, based on the tunneling process proposed above. A similar expression for I_{DT} is available in the literature, and is reproduced here for completeness.

For simplicity, the expressions presented assume a constant effective electron mass throughout the tunneling process and the WKB approximation for the tunneling probabilities. Further, we assume a triangular approximation for the potential barrier shape, which is justified since the percentage change in the electric field over the barrier thickness
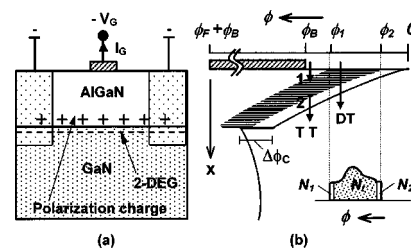

FIG. 1. (a) Device structure and biasing arrangement. (b) Energy band diagram from gate to substrate, showing the tunneling processes, trap band ($\phi_2 \leq \phi \leq \phi_1$), and critical energy parameters. Also shown is the distribution of trap concentration N_t over energy.

[a]Electronic mail: skarmalkar@hotmail.com
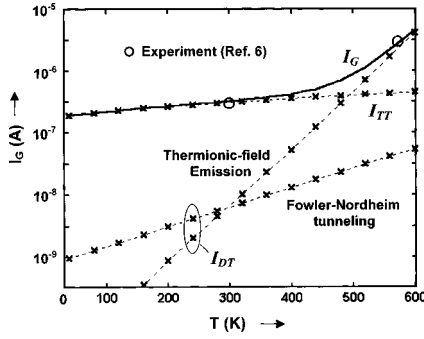[b]Electronic mail: shurm@rpi.edu

FIG. 2. Calculated I_G vs T behavior based on the proposed model. The calculations are for the device No. 2 of Fig. 3 and Table I, at $V_G = |V_T| = 2.4$ V or $E = 1.76$ MV/cm.

through which tunneling occurs is small. This is because, the barrier thickness is a fraction of the AlGaN layer width, d, and a significant portion of the field in the AlGaN layer comes from the polarization sheet charge at the heterojunction. Therefore, the barrier electric field E can be assumed to be the equal to the peak field at the gate junction, so that

$$E = \frac{V_G + V_0}{d} \quad \text{for} \quad V_G \leq |V_T|,$$

$$V_0 = \phi_B - \Delta\phi_C - \phi_{fb} + qN_d d^2/2\varepsilon. \tag{2}$$

Here, ϕ_B is the barrier height, $\Delta\phi_c$ is the heterojunction conduction band discontinuity, ϕ_{fb} is the difference between the conduction band edge and the Fermi-level in the substrate, and N_d is the AlGaN layer doping. E is assumed to saturate for $V_G \geq |V_T|$.[5]

I_{TT} is derived as follows. The probabilities P_1 and P_2 of the two tunneling processes 1 and 2 (see Fig. 1) are given by[7]

$$P_1 = \exp\left\{-\frac{\alpha}{E}[\phi^{3/2} - (\phi_1 - \psi)^{3/2}]\right\},$$

$$P_2 = \exp\left[-\frac{\alpha}{E}(\phi_2 + \psi)^{3/2}\right], \quad \alpha = \frac{8\pi\sqrt{2mq}}{3h}. \tag{3}$$

These decay rapidly for energies, ψ, away from the band edges $\phi_{1,2}$ into the band, so that the actual trap distribution over energy can be replaced by effective trap densities $N_{1,2}$ located at $\phi_{1,2}$ (in analogy to the well known concept of effective density of conduction and valence band states, Nc, v). Note that, the effective trap density concept allows any arbitrary shape for the trap distribution over energy (see Fig. 1) and distance. Equally important is its implication that, only the trap distribution near the trap band edge, rather than the distribution over the entire band, is of significance.

In our work, we assume a uniform trap concentration, N_t, over distance as well as energy, because the exact shape of the trap distribution in the experimental devices of our letter is not known at this time. Even if the actual trap distribution turns out to be nonuniform, our results based on the uniform distribution assumption have significance as an effective description of the physical situation, and do not affect the intrinsic validity of our model. For the uniform trap concentration assumed, we can write

$$N_{1,2} = \frac{N_t}{(\phi_1 - \phi_2)}\left(\int_0^{\phi_1 - \phi_2} P_{1,2}d\psi/P_{1,2}^0\right),$$

$$P_{1,2}^0 = P_{1,2}|_{\psi=0}. \tag{4}$$

Using the effective trap density transformation, the I_{TT} is readily modeled by an adaptation of the TT model based on a single trap level, available in literature.[7,8] The tunneling rates are written as $R_1 = C_1 f_{FD}(1 - f_t)N_1 P_1^0$ and $R_2 = C_2 f_t N_2 P_2^0$. Here, f_{FD} is the temperature dependent Fermi–Dirac occupancy fraction in the metal and $C_{1,2}$ is trap energy dependent rate constant,[7] given by

$$f_{FD} = \frac{1}{1 + \exp[(\phi_B - \phi)/V_t]},$$

$$C_{1,2} = \frac{16\pi q E_1^{3/2}}{3h\sqrt{\phi_{1,2} - E_1}}, \quad E_1 = 0.2 \text{ V.} \tag{5}$$

I_{TT} is obtained by deriving f_t using the steady state condition $R_1 = R_2$, and integrating the tunneling rate $R = R_1 = R_2$ over the AlGaN layer width,[7,8] employing the transformation $dx = (d\phi/E)$, i.e.,

$$I_{TT} = \frac{qS}{E}\int_{\phi_2}^{\phi_B + \phi_F} R\,d\phi,$$

$$\frac{1}{R} = \frac{1}{C_1 f_{FD}N_1 P_1^0} + \frac{1}{C_2 N_2 P_2^0},$$

$$P_1^0 = 1 \quad \text{for} \quad \phi_2 \leq \phi \leq \phi_1, \tag{6}$$

where S denotes the gate area.

I_{DT} is calculated as the larger of the two values predicted by the Fowler–Nordheim (FN) expression[9] which dominates at low temperatures (see Fig. 2):

$$I_{DT}^{FN} = \frac{q^2 SE^2}{8\pi h\phi_B}\exp\left(-\frac{\alpha}{E}\phi_B^{3/2}\right) \tag{7}$$

and the thermionic field emission (TFE) expression[5]

$$I_{DT}^{TFE} = \frac{qSA^*T}{k}\int_0^{\phi_B} f_{FD}P\,d\phi, \quad P = \exp\left(-\frac{\alpha}{E}\phi^{3/2}\right). \tag{8}$$

Here, A^* is the Richardson constant, and other symbols have their usual meanings.

In this work, we obtained I_G using a numerical evaluation of the integrals in Eqs. (6) and (8). A completely analytical approach of determining I_G will be discussed in a subsequent work. The primary parameters in our model are ϕ_B, ϕ_1, ϕ_2, N_t, and V_0. In current evaluation using Eqs. (6)–(8), except in V_0 calculation, we incorporated the ϕ_B lowering due to image force[9] and band gap reduction with temperature,[10,11] as per the relation

$$\phi_B = \phi_{B0} - \gamma_1\sqrt{\frac{q}{4\pi\varepsilon}}\sqrt{E} - \gamma_T T. \tag{9}$$

γ_T, γ_1 and the effective mass m are the three secondary parameters in our model. For a given device, the parameters are fitted by a systematic procedure. Values of ϕ_{B0}, V_0, m, γ_1, and γ_T are assumed based on material properties. Next, the values of trap parameters N_t, ϕ_1, and ϕ_2 are adjusted by noting that their increase has the following effect on the I_G–V_G curve: upward shift in case of N_t; upward shift and reduced temperature dependence at high V_G, in case of ϕ_1; downward and anticlockwise movement, and reduced tem-
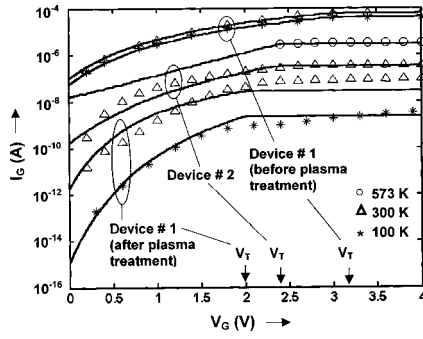
FIG. 3. Model fit (solid lines) to experimental data (points) using the parameters shown in Table I, $m=0.17m_0$, $\gamma_1=0.4$, and $\gamma_T=2.7 \times10^{-4}$ V/K. For device No. 1, $d=200$ Å and $S=1.1\times100$ μm^2 (see Ref. 3), and for device No. 2, $d=250$ Å and $S=1\times100$ μm^2 (see Ref. 6). For device No. 2 at 573 K only saturation data is available in Ref. 6.

perature dependence at low V_G, in case of ϕ_2. This procedure is iterated by minor modifications in the values of ϕ_{B0}, V_0, m, γ_1, and γ_T, and then in N_t, ϕ_1, and ϕ_2, until best model fit to experiment is obtained.

First, we consider the experimental I_G–V_G data of a HEMT before and after plasma treatment, reproduced here in Fig. 3 (device No. 1), from Ref. 3. Prior to the treatment, $|V_T|=3.2$ V, and the current is high and almost insensitive to temperature between 100 and 300 K. After treatment, $|V_T|$ reduces to 2 V; the saturation I_G is suppressed but becomes sensitive to temperature, increasing by a factor of $\sim$30 from 100 to 300 K. We apply our model and parameter extraction procedure to this data, with initial assumptions of $\phi_{B0}=1.4$ V (see Ref. 3), $V_0=1.6$ V (using $\Delta\phi_c=0.4$ V, $\phi_{fb}=0.2$ V, $\epsilon=8.9$, $N_d=2\times10^{18}$ cm^{-3} and $d=200$ Å), $m=0.17m_0$ (average of $0.1m_0$ in the metal[8] and $0.23m_0$ in AlGaN),[12] $\gamma_1=0.4$ (40% of the value used in thermionic emission calculations),[9] and $\gamma_T=2.7\times10^{-4}$ V/K (band gap reduction in AlGaN).[12] We obtain the parameter values given in Table I, and a good fit to the experimental data (see Fig. 3). The trap band is located $\sim$0.4 V below the conduction band edge. Plasma treatment does not affect this location, but reduces the trap bandwidth from $\sim0.7\phi_{B0}$ to $\sim0.5\phi_{B0}$, i.e., by $\sim$0.25 V, and suppresses N_t by $\sim$100 times. This along with the $|V_T|$ reduction is responsible for the decrease in gate current. The bandwidth reduction due to a decrease in ϕ_1 causes the increased temperature dependence of I_G. The reduction in V_0 after plasma treatment is due to the reduction in N_d, which accounts for a part of the observed reduction in $|V_T|$ (the remaining reduction comes from change in the polarization charge).

Following observations from our extensive curve fitting

trials provide further rationalization of the changes due to plasma treatment measured by our model. It is impossible to obtain a fit for the plasma treated device, without reducing N_t as compared to that before plasma treatment (see Table I), implying that plasma treatment definitely reduces N_t. A fit can be obtained for the plasma treated device using the same trap bandwidth as that before plasma treatment, by increasing ϕ_B to 1.6 V. However, we ignored this alternative, since, if the plasma treatment affects the trap concentration, it is likely to affect the bandwidth as well, and on the other hand, we do not have a plausible explanation for the increase in barrier height by plasma treatment. Further independent investigations are required to reveal the mechanism of the changes due to plasma.

Our model shows that, the device current at 100 and 300 K is dominated by TT, independent of the processes such as plasma treatment used in device fabrication. To illustrate that the DT current becomes important at higher temperatures, we consider another device (No. 2) whose measured I_G rises by an order of magnitude from 300 to 573 K (see Ref. 6). Figure 3 shows that our model successfully predicts this reported I_G data using the parameters of Table I. Figure 2 shows that, while the TT current dominates at 300 K (as in device No. 1), the DT current dominates at 573 K.

Earlier models of AlGaN gate leakage (e.g., Ref. 5), have assumed TFE to be the main mechanism at all temperatures, and attributed the discrepancies between the model predictions and measurements to the effect of traps. Further, it has been suggested[3] that traps influence direct tunneling between gate and the channel by altering the gate depletion width, i.e., tunneling barrier thickness. This requires that N_t be comparable to N_d. Our work has clearly exposed the weakness in these approaches by showing that, TT is the main current mechanism for $T<500$ K, in spite of N_t being orders of magnitude less than N_d (thereby having negligible effect on the depletion width).

In conclusion, we gave the mechanism of the reverse gate current in AlGaN/GaN HEMTs, clearly illustrating the nature of traps in the AlGaN layer and the extent of their assistance to the electron tunneling from the gate to substrate, at different temperatures and voltages.

TABLE I. Extracted model parameters.

Device No.	ϕ_{B0} (V)	V_0 (V)	ϕ_1 (V)	ϕ_2 (V)	N_t (cm^{-3})
1[a]	1.4	1.6	1.35	0.45	1.7×10^{15}
1[b]	1.4	1.0	1.11	0.45	1.5×10^{13}
2	1.32	2.0	1.3	0.55	1.0×10^{14}

[a]Before plasma treatment.
[b]After plasma treatment.

[1] Y. F. Wu, B. P. Keller, P. Fini, S. Keller, T. J. Jenkins, L. T. Kehias, S. P. DenBaars, and U. K. Mishra, IEEE Electron Device Lett. **19**, 50 (1998).
[2] S. Karmalkar, J. Deng, M. S. Shur, and R. Gaska, IEEE Electron Device Lett. **22**, 373 (2001).
[3] S. Mizuno, Y. Ohno, S. Kishimoto, K. Maezawa, and T. Mizutani, Jpn. J. Appl. Phys., Part 1 **41**, 5125 (2002).
[4] M. E. Levinshtein, S. L. Rumyantsev, R. Gaska, J. W. Wang, and M. S. Shur, Appl. Phys. Lett. **73**, 1089 (1998).
[5] E. J. Miller, X. Z. Dang, and E. T. Yu, J. Appl. Phys. **88**, 5951 (2000).
[6] M. S. Shur, A. D. Bykhovski, R. Gaska, and A. Khan, in *Handbook of Thin Film Devices, Volume 1: Hetero-structures for High Performance Devices*, edited by M. H. Francombe (Academic, San Diego, 2000), p. 299.
[7] X. R. Cheng, Y. C. Cheng, and B. Y. Liu, J. Appl. Phys. **63**, 797 (1988).
[8] C. Svensson and I. Lundstrom, J. Appl. Phys. **44**, 4657 (1973).
[9] A. van der Ziel, *Solid State Physical Electronics* (Prentice-Hall, India, 1971).
[10] E. H. Rhoderick and R. H. Williams, *Metal-Semiconductor Contacts* (Clarendon, Oxford, 1978).
[11] R. Hackam and P. Harrop, Solid State Commun. **11**, 669 (1972).
[12] V. Bougrov, M. Levinshtein, S. Rumyantsev, and A. Zubrilov, in *Properties of Advanced Semiconductor Materials*, edited by M. E. Levinshtein, S. L. Rumyantsev, and M. S. Shur (Wiley, New York, 2001), p. 1.